2,4,5-Trihydroxyphenylalanine Quinone Biogenesis in the Copper Amine Oxidase from *Hansenula polymorpha* with the Alternate Metal Nickel[†]

Nicole M. Samuels and Judith P. Klinman*

Department of Chemistry and Department of Molecular and Cell Biology, University of California, Berkeley, California 94720

Received June 19, 2005; Revised Manuscript Received August 25, 2005

ABSTRACT: Copper amine oxidase (CAO) is a dual-functioning enzyme that catalyzes the biosynthesis of a self-derived coenzyme and subsequent oxidative deamination of primary amines. The organic cofactor, 2,4,5-trihydroxyphenylalanine quinone (TPQ), is generated from the post-translational modification of an active site tyrosine (Y405) in a reaction shown to be dependent on both molecular oxygen and a mononuclear copper center. Previous investigations of Cu(II)-dependent cofactor formation in the *Hansenula polymorpha* amine oxidase (HPAO) provided evidence for the coordination of the precursor tyrosine in forming a ligand-to-metal charge transfer complex as a means of activating the tyrosyl ring for direct attack by triplet-state dioxygen. To further delineate the role of the metal in facilitating this complex series of reactions, apo-HPAO was reconstituted with alternate metals of varying reduction potentials and Lewis acidities [Ni(II), Co(II), Mn(II), Fe(II), and Fe(III)] and the consequence of each substitution on TPQ biogenesis examined. Ni(II) was found to support the transformation of the precursor tyrosine to the quinone cofactor to yield a mature enzyme competent for methylamine oxidation. Detailed kinetic analysis of the mechanism of TPQ biogenesis for the Ni(II)-substituted enzyme has led to the proposal of a direct electron transfer from the metal-coordinated tyrosinate to dioxygen as the dominant rate-limiting step.

Copper amine oxidase (CAO)[1] catalyzes the two-electron oxidative deamination of primary amines to the corresponding aldehyde and ammonia coupled with the reduction of dioxygen to hydrogen peroxide (*1*). CAOs are ubiquitous in nature and have proposed biological functions that are as diverse as the myriad of host organisms in which the enzyme is found (*2*). In yeast and bacteria, CAO serves as a catabolic enzyme to provide a source of nitrogen and carbon. However, in mammals, CAO has been proposed to play a role in the metabolism of glucose and the trafficking of leukocytes, being implicated in diseases such as diabetes and atherosclerosis (*3*).

All CAOs house two redox cofactors: a mononuclear copper(II) center and the organic cofactor, 2,4,5-trihydroxyphenylalanine quinone (TPQ). Besides utilizing both cofactors to catalyze amine oxidation, the enzyme must also synthesize the covalent quinone cofactor de novo. CAO is a member of a select group of bifunctional enzymes that contain "homemade cofactors" that are derived from the post-translational modification of specific active site residues. In the case of CAO, a precursor tyrosine located within the highly conserved consensus sequence (N-**Y**-D/E-Y) is converted to TPQ by an autocatalytic mechanism termed cofactor biogenesis (*4*, *5*). This transformation does not require the aid of any auxiliary enzymes or external reducing equivalents (*6*). The processing of the precursor tyrosine to TPQ is solely dependent on the presence of dioxygen and a functional copper center (*7*).

Over the years, several mechanisms have been proposed for the overall six-electron oxidation of tyrosine to TPQ in CAO. On the basis of the collective results of crystallographic (*8*, *9*), stoichiometric (*6*), kinetic (*10*, *11*), and spectroscopic studies (*12*, *13*), a consensus mechanism for the Cu(II)-dependent formation of TPQ has emerged. Key to this mechanism is the reaction between dioxygen and the "activated" precursor tyrosine in the form of a tyrosinate−Cu(II) ligand-to-metal charge transfer (LMCT) complex (*11*, *12*). Due to the nature of the oxygen−copper bond in this complex, partial radical character is imparted onto the tyrosyl ring, which circumvents the spin-forbidden nature of the direct reaction between the tyrosine and triplet dioxygen (*14*). Experimental evidence for the LMCT complex comes from the observation of a spectral intermediate (350 nm) that forms rapidly upon aeration of the Cu(II)−enzyme complex and subsequently decays in a manner concomitant with the appearance of TPQ (*12*, *15*). The 350 nm intermediate represents the species that reacts with the first mole of oxygen, the rate-limiting step in Cu(II)-catalyzed TPQ biogenesis. Crystal structures of the Zn(II) and Cu(II) forms

[†] This work was supported by a National Institutes of Health Grant (GM 039296) to J.P.K. and a National Institutes of Health postdoctoral fellowship (F32 GM64215) to N.M.S.

* To whom correspondence should be addressed. Telephone: (510) 642-2668. Fax: (510) 643-6232. E-mail: klinman@berkeley.edu.

[1] Abbreviations: AGAO, *Arthrobacter globiformis* amine oxidase; ARD, aci-reductone dioxygenase; CAO, copper amine oxidase; dopa, 3,4-dihydroxyphenylalanine; EPR, electron paramagnetic resonance; HEPES, *N*-(2-hydroxyethyl)piperazine-*N*′-2-ethanesulfonic acid; HPAO, *H. polymorpha* amine oxidase; ICP-AES, inductively coupled plasma-atomic emission spectroscopy; KIE, kinetic isotope effect; LMCT, ligand-to-metal charge transfer; MALDI, matrix-assisted laser desorption ionization; MomA, quinone-forming monooxygenase; topa, 2,4,5-trihydroxyphenylalanine; TPQ, 2,4,5-trihydroxyphenylalanine quinone; WT, wild type.

10.1021/bi051176m CCC: $30.25
Published on Web 10/05/2005

of CAO, where the hydroxyl oxygen of the precursor tyrosine is axially bound to the metal and poised for monooxygenation, provide support for the intermediacy of a LMCT complex (*8*, *9*). Further, quantum mechanical calculations of the mechanism for cofactor formation are consistent with experimental data showing that the largest overall barrier involves the addition of the first oxygen atom to the precursor tyrosine (*16*). In total, these data highlight the level of difficulty for the monooxygenation of tyrosine and the importance of the neighboring mononuclear copper center in TPQ biogenesis.

As the requirement for copper appeared to be absolute, we have assessed the impact of alternate metals with varying electronic properties on cofactor formation. Earlier studies had indicated that divalent metals other than Cu(II) were inert (*17*), consistent with the presence of Tyr at position 405 in the zinc-substituted enzyme (*8*). In this study, the apo form[2] of the *Hansenula polymorpha* amine oxidase (HPAO) was prepared and reconstituted with an array of transition metals in an effort to identify those that allow for TPQ biogenesis. Herein, we demonstrate that Ni(II) is a catalyst for cofactor formation in HPAO and report the detailed kinetic analysis of the Ni(II)-catalyzed reaction to assess the role of this metal in the monooxygenation of the precursor tyrosine and other important steps in TPQ biogenesis. We provide evidence that the hydration of the 3,4-dihydroxyphenylalanine (dopa) quinone intermediate by a Ni(II)-bound hydroxide ion is likely to be a partially rate-limiting step in TPQ biogenesis. The data collectively point toward the initial oxidation of the Ni(II)−tyrosinate complex by dioxygen as a major rate-limiting step in Ni(II)-catalyzed cofactor formation. The enhancement of dioxygen reactivity toward the precursor tyrosine in the context of a mononuclear nickel center is discussed.

EXPERIMENTAL PROCEDURES

Materials. HEPES, pyrogallol, Chelex 100, and casein were obtained from Sigma. $ZnCl_2$ and $NiCl_2$ (>99.9999%) were purchased from Aldrich. Phenylhydrazine and 3,5-[$^2H_2$]-tyrosine (98%) were purchased from Fluka and Cambridge Isotopes, respectively.

Subcloning, Expression, and Purification of Apo-HPAO. The pKW3 construct (*7*) harboring the WT HPAO gene was digested with *Nde*I and *Bam*HI, and the fragment was ligated into the appropriate sites of a pET3a vector (Novagen). The Y405V mutant of HPAO was prepared using a Quik Change II site-directed mutagenesis kit (Stratagene) and the primers 5′-CAA ATA TTT ACT GCT GCC AAT GTC GAG TAC TGT CTG TAC TGG-3′ and 5′-CCA GTA CAG ACA GTA CTC GAC ATT GGC AGC AGT AAA TAT TTG-3′, where the mutated codons are underlined. The BL21(DE3) *Escherichia coli* expression strain was transformed with the resulting pET3a construct and grown on LB-ampicillin agar. Apo-HPAO was overexpressed and purified by methods previously described (*12*) with slight modifications. Metal-free medium (~150 mL) was inoculated with a single colony and shaken at 37 °C until the culture reached a final A_{600} of ~0.6. The starter culture was stored overnight at 4 °C and used to inoculate plastic Fernbach flasks containing 1.5 L of metal-free medium the following day. Typically, the large cultures were grown to an A_{600} of ~0.6, and protein expression was induced with 0.4 mM IPTG. As a final step, metal chelators were removed from purified HPAO by buffer exchange into 50 mM HEPES (pH 7.0) using a 30 000 molecular weight cutoff (MWCO) ultracentrifuge (Millipore). Protein concentrations were determined by the Bradford assay (Bio-Rad), and purified HPAO stocks (~20 mg/mL) were stored at −20 °C.

Preparation of Anaerobic Samples. All samples were made anaerobic in septa-covered vessels by exchanging dissolved air with argon gas that had been scrubbed of oxygen by a basic solution of pyrogallol. For the buffer or $NiCl_2$, argon was bubbled directly through the solution for at least 1 h. Alternatively, apo-HPAO or Zn(II)-HPAO was maintained on ice, and a steady stream of argon gas was passed over the top of the protein solution for at least 1 h. To prevent contamination by minute amounts of aerosolized pyrogallol, a dry ice trap was placed between the sparger containing the scrubbing solution and the sample.

Spectral Analysis of Binding of Ni(II) to Apo-HPAO and Cofactor Formation. Metal binding and TPQ biogenesis events were monitored on a Hewlett-Packard 8452A diode array spectrophotometer with a thermostated cell holder maintained at 25 °C. Solutions of $NiCl_2$, apo-HPAO, and Zn(II)-HPAO were made anaerobic in separate vessels, and Ni(II) was delivered to the protein via a gastight syringe. Spectral changes accompanying the binding of Ni(II) to apo-HPAO or Zn(II)-HPAO in the absence of oxygen were measured during a 2 h incubation. Absorbance features attributed to Ni(II) bound to HPAO in the absence of oxygen were subtracted electronically; subsequent cofactor biogenesis was initiated by passing a stream of compressed air or oxygen over the protein solution for 6 min with gentle swirling. The topa and dopa quinones were detected by reaction at various times with phenylhydrazine. All absorbance values were normalized to the average baseline between 750 and 800 nm. The observed rate constants were determined with a fit to a single exponential using KaleidaGraph 3.0.2.

Metal Binding Stoichiometry. Anaerobic solutions of HPAO and $NiCl_2$ were prepared separately and immediately transferred to a glovebox. A molar equivalent of metal was incubated with apo-HPAO at 25 °C for 2 h, and the unbound Ni(II) was removed by washing the protein with anaerobic buffer in a 50 000 MWCO ultrafilter (Millipore). The total amount of metal bound was measured by inductively coupled plasma-atomic emission spectroscopy (ICP-AES) on an Optima 3000 DV instrument (Perkin-Elmer).

EPR. Electron paramagnetic resonance spectra were recorded on a Varian E-109 spectrometer with an E-102 microwave bridge and an X-band resonator. The spectrometer was equipped with an Air Products Heli-tran liquid helium cryostat, and the spectra were acquired at 6 K. Apo-HPAO and metal stock solutions were made anaerobic and immediately transferred to a glovebox, where the protein was reconstituted with 1 equiv of $NiCl_2$. Following a 2 h incubation, the Ni(II)-bound protein was washed with anaerobic buffer to remove unbound metal as described in Metal Binding Stoichiometry. The Ni(II)-HPAO sample was

[2] Apoenzyme refers to a metal-free protein in which the precursor tyrosine (Y405) is unprocessed. Mature enzyme refers to a protein containing metal in which the precursor tyrosine has been converted to TPQ.

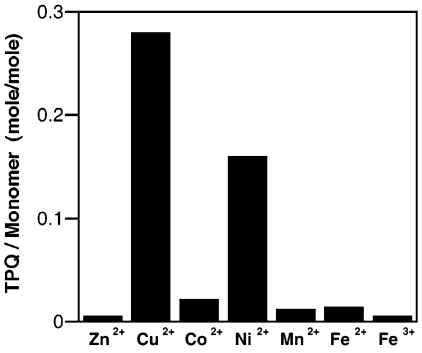

FIGURE 1: Reconstitution of apo-HPAO with alternate metals. Quantification of TPQ from a 2 week incubation at 4 °C by an end point assay reaction with phenylhydrazine.

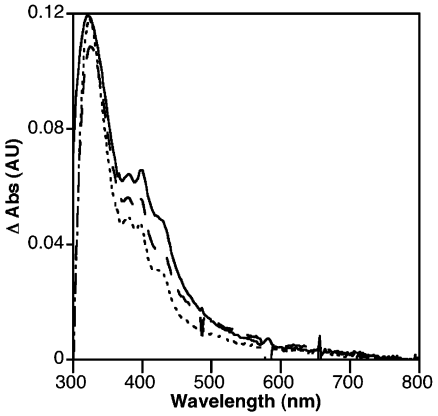

FIGURE 2: Ni(II)-dependent spectral changes. Difference spectra following the incubation of 1 equiv of $NiCl_2$ with WT apo-HPAO (—), Zn(II)-HPAO (— — —), and apo-Y405V (- - -) for 2 h in the absence of oxygen. Absorbance features for the apoenzyme and Zn(II)-bound enzyme prior to the addition of $NiCl_2$ have been subtracted. Reactions were performed under the following conditions: 40 μM HPAO, 46 μM Zn(II), and 40 μM Ni(II) in 50 mM HEPES at pH 8.1 and 25 °C.

then removed from the glovebox and aerated for 6 min by a steady stream of house air. At the designated times, an aliquot (250 μL) was transferred to an EPR tube (Wilmad Glass, Buena, NJ) and immediately frozen in 2-methylbutane that had been cooled to liquid nitrogen temperature. EPR signal quantitation was performed using the Cu(II)−EDTA species as a spin standard.

Steady-State Kinetic Analysis of Metal-Reconstituted HPAO. Apo-HPAO was reconstituted with Ni(II) or Cu(II) and allowed to produce TPQ over a 45 h incubation at 25 °C in air-saturated 50 mM HEPES (pH 8.1). The cofactor-containing protein was washed with buffer to remove unbound metal and assayed for methylamine oxidation using the method reported previously (*18*).

Preparation of 3,5-[$^2H_2$]Tyrosine-Containing Apo-HPAO. Procedures for the preparation of HPAO containing labeled tyrosine have been described previously (*13*). Briefly, BL21-(DE3) cells harboring the WT-HPAO-pET3A construct were grown in defined metal-free medium containing all amino acids except tyrosine. At the time of induction, 3,5-[$^2H_2$]-tyrosine was added to the cultures to a final concentration of 200 mg/L. The degree of incorporation of labeled tyrosine was determined by digestion of apo-HPAO (100 μg) with trypsin (2 μg) for 24 h at 30 °C. The peptide mixture was analyzed by matrix-assisted laser desorption ionization (MALDI) mass spectrometry on a Voyager-DE Pro spectrometer (Applied Biosystems).

RESULTS

Reconstitution of HPAO with First-Row Transition Metals. In an initial survey, apo-HPAO was reconstituted with 1 equiv of each metal and the final amount of cofactor generated during an extended incubation was quantified by reaction with the quinone reactive reagent, phenylhydrazine (ϵ_{448} = 40.5 mM^{-1} cm^{-1}) (*19*) (Figure 1). Consistent with earlier observations for TPQ derived from HPAO that had been reconstituted with Cu(II) *in vitro*, the final yield of cofactor was in the range of 25−30% as judged by an end point assay. Surprisingly, Ni(II) catalyzed the oxidation of the precursor tyrosine (Y405) to TPQ under air saturation. Although previous investigations established that Co(II) could sufficiently replace Cu(II) in the oxidation of methylamine to formaldehyde (*20*, *21*), the cobaltous ion did not support cofactor formation in HPAO to a significant extent. Therefore, thorough kinetic analyses were performed to determine the mechanism by which the mononuclear Ni(II) center catalyzes the transformation of the precursor tyrosine into TPQ.

Binding of Ni(II) to Apo-HPAO. To better decipher the mechanism for cofactor formation in the Ni(II)-substituted enzyme, apo-HPAO was reconstituted with a stoichiometric amount of Ni(II) under anaerobic conditions and the amount of metal retained by the protein was quantified by ICP-AES after washing to remove unbound and weakly bound metal. At pH 7.0, only 0.45 equiv of Ni(II) was bound to HPAO following a 2 h incubation in the absence of oxygen. Increasing the pH to 8.1 led to the retention of 0.70 equiv of Ni(II), and all subsequent studies were performed at this pH to ensure that the majority of the nickel present was protein-bound. Concurrent with the anaerobic addition of 1 equiv of Ni(II) to apo-HPAO, a broad absorbance feature (300−600 nm) appeared over time (Figure 2). The addition of Ni(II) to either an enzyme sample that had been previously bound with 1 equiv of Zn(II) or the apo-Y405V mutant under the same conditions revealed similar optical features (Figure 2).

Cofactor Formation in Ni(II)-HPAO. The rate constant for the formation of the cofactor (k_{TPQ}) was measured spectrophotometrically following the aeration of Ni(II)-reconstituted HPAO. Figure 3A shows the difference spectra for this reaction minus the absorbance signal that had been previously shown to arise solely from Ni(II) bound to the enzyme in the absence of oxygen (Figure 2). Two species appeared at 334 and 480 nm (λ_{max}), with rate constants of 0.085 and 0.028 h^{-1}, respectively (Table 1); the species at 480 nm represents TPQ. Although the 334 nm species was kinetically competent to be a chemical intermediate, it did not display a precursor−product relationship with respect to the newly formed cofactor peak. Moreover, aeration of the Ni(II)-bound Y405V mutant, which is incapable of producing TPQ, under identical conditions also yielded a broad absorbance feature with a λ_{max} of 334 nm (Figure 3B). The observed rate constant for cofactor formation in Ni(II)-HPAO was found to be dependent on the concentration of dissolved oxygen. The introduction of 100% oxygen to Ni(II)-HPAO did not result in any

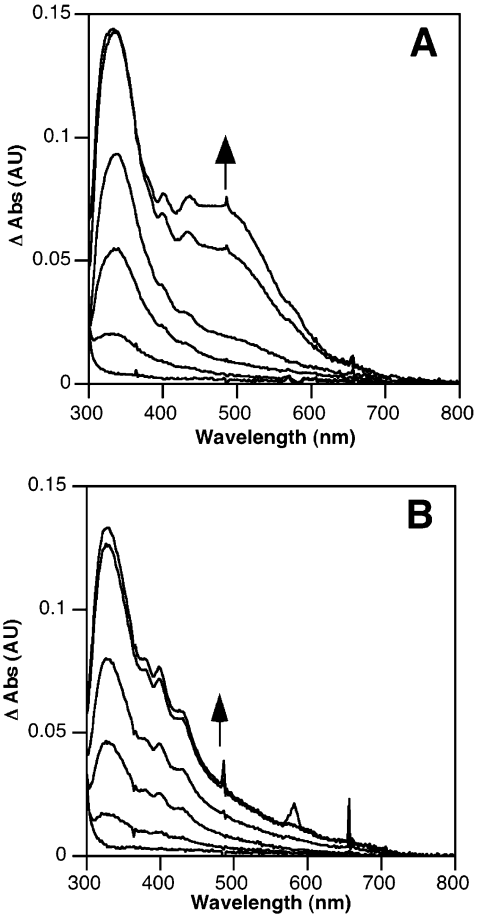

FIGURE 3: O_2-dependent spectral changes. (A) Difference spectra following the aeration of WT Ni(II)-HPAO. (B) Difference spectra following the aeration of Ni(II)-Y405V. Spectra are shown 0, 1, 4, 10, 35, and 58 h following aeration. All absorbance features prior to the addition of oxygen were subtracted. Reactions were performed under the following conditions: 40 μM HPAO and 40 μM Ni(II) in 50 mM HEPES at pH 8.1 and 25 °C.

Table 1: Kinetic Properties of HPAO Reconstituted with Cu(II) and Ni(II)[a]

	k_{TPQ}[b,c] with air (h^{-1})	k_{TPQ}[b,d] with O_2 (h^{-1})	$^2H_2$ k_{TPQ}[b,c,e] with air (h^{-1})	k_{cat}[c,f] with air (s^{-1})
Cu(II)	3.3 (0.6)	–	–	3.80 (0.06)
Ni(II)	0.028 (0.006)	0.044 (0.009)	0.031 (0.006)	0.09 (0.01)

[a] All reactions were conducted in 50 mM HEPES at pH 8.1 and 25 °C. [b] Measured at 480 nm with 40 μM HPAO and 40 μM Ni(II). Shown in parentheses are the standard deviations from three separate determinations. [c] Reactions performed in air-saturated buffer. [d] Reactions performed in oxygen-saturated buffer. [e] Reactions assessed for HPAO containing 3,5-[$^2H_2$]tyrosine. [f] Methylamine oxidation measured by the oxygen electrode assay with protein concentrations of <0.5 μM. Numbers in parentheses represent the standard error for fits to the Michaelis–Menten equation.

overall changes in the UV–vis spectra (data not shown); however, cofactor was generated at a rate of 0.044 h^{-1} (Table 1). Curiously, the 334 nm species also had a strong dependence on the oxygen concentration (data not shown) and ultimately was ascribed to the product of an oxygen-dependent reaction between the protein and nickel that was off the reaction path from TPQ biogenesis.

To determine the oxidation state of the nickel ion and detect the presence of an organic radical during the transformation of the precursor tyrosine to TPQ in Ni(II)-HPAO,

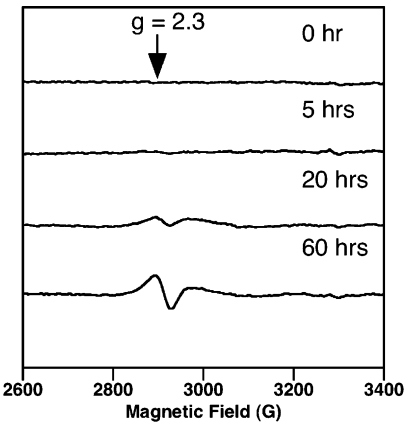

FIGURE 4: X-Band EPR spectra of Ni(II)-HPAO during cofactor biogenesis. Spectra were collected 0, 5, 20, and 60 h following aeration of Ni(II)-HPAO. A blank spectrum (water) has been subtracted from each protein spectrum. Final conditions: 43 μM HPAO and 50 mM HEPES at pH 8.1. Instrument parameters: microwave frequency, 9.245 GHz; modulation amplitude, 25 G; microwave power, 1 mW; time constant, 0.5 s; temperature, 6 K; and two scans averaged.

the EPR spectrum of the protein was recorded at various times throughout the course of the reaction (Figure 4). A solitary organic radical was not observed at any point during Ni(II)-catalyzed TPQ biogenesis as indicated by the absence of a single axial peak at $g = 2.0$. However, a weak signal at $g = 2.3$ slowly emerged that was consistent with either a Ni(III) (*22*, *23*) or an antiferromagnetically coupled Ni(II)–phenoxyl radical species (*24*). Since the minor EPR active species (~0.5 μM unpaired spin in relation to 15 μM TPQ formed) did not appear to behave as a biogenic intermediate, it was assigned as an end product of a side reaction that was not on the path to TPQ formation. The bulk of the nickel present during the transformation of tyrosine to TPQ was EPR silent, a state consistent with Ni(II). On the basis of these observations and those described above, together with the proposed mechanism for Cu(II)-dependent biogenesis (*25*), a working mechanism for Ni(II)-catalyzed cofactor formation in HPAO was put forth (Scheme 1).

Rate-Limiting Step in Ni(II)-Catalyzed Cofactor Formation. Compared to that with Cu(II), the rate constant for Ni(II)-catalyzed TPQ biogenesis in air-saturated buffer (pH 8.1) is 120-fold slower (Table 1). Given the different reduction potentials for oxygen and nitrogen complexes of Cu(II) [+0.12 V vs NHE (*26*)] versus Ni(II) [−1.16 V vs NHE (*27*)] and the fact that aquo Ni(II) ($pK_a = 9.4$) is a weaker Lewis acid than aquo Cu(II) ($pK_a = 7.5$) (*28*), the exchange could potentially impact the microscopic rate constants for several steps during cofactor formation in HPAO.

To start, the rate of Ni(II)-promoted oxidase activity during the catalytic cycle of amine oxidation can be used to shed light on the nature of rate-limiting steps during TPQ biogenesis. First, the turnover number for amine oxidation sets a lower limit on the rate constant for the oxidation of the aminoquinol to TPQ (Scheme 2). Second, the reduction potentials for the aminoquinol and quinol forms of the cofactor are expected to be similar (*29*) and, hence, their rates of oxidation. As shown in Table 1, reconstitution of apo-HPAO with Ni(II) to produce mature enzyme led to a k_{cat} of 0.09 s^{-1} for the oxidation of methylamine, a value 10^4 faster than the k_{TPQ} for Ni(II)-HPAO. This comparison

Scheme 1: Proposed Mechanism for TPQ Biogenesis in Ni(II)-HPAO[a]

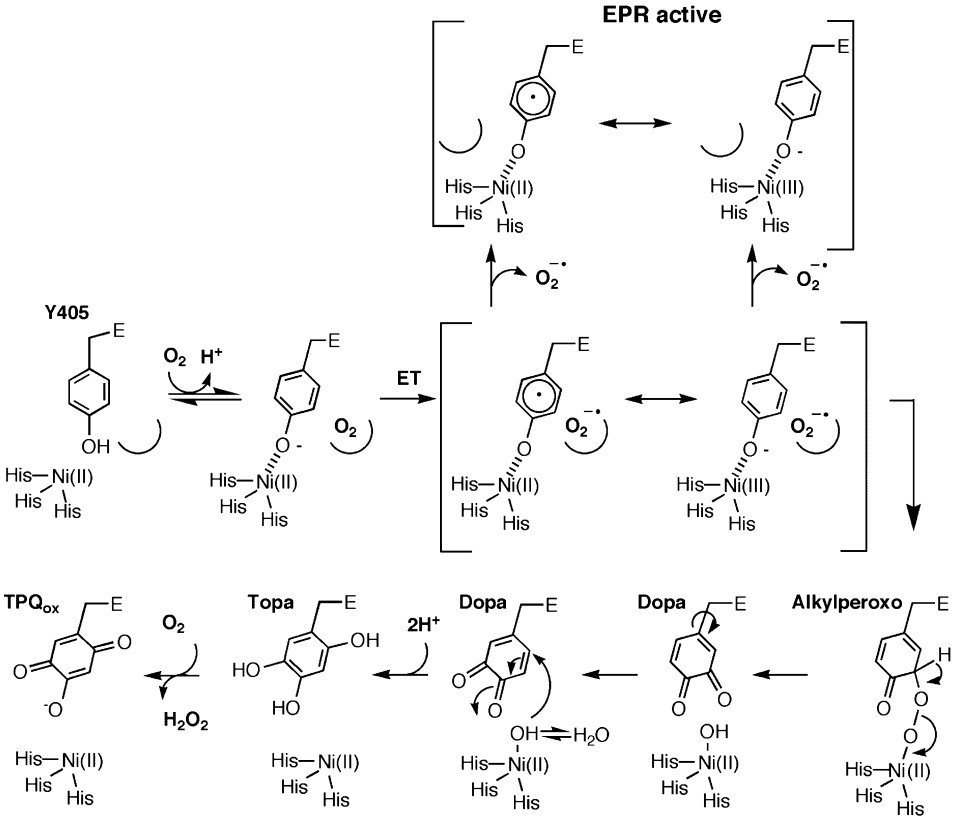

[a] Water ligands to the metal have been omitted for simplicity. The mature Ni(II)-substituted AGAO has been shown to have octahedral geometry with the three conserved histidines bound axially and water ligands completing the octahedron (*34*).

Scheme 2: Comparison of Oxidation of Trihydroxyphenylalanine versus Aminoquinol

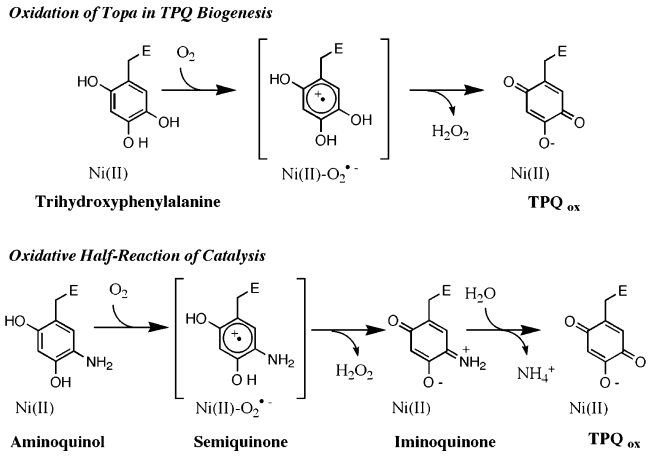

argued strongly against a rate-limiting oxidation of 2,4,5-trihydroxyphenylalanine (topa) in the course of the biogenesis of TPQ with the Ni(II)-reconstituted enzyme.

To assess the impact of the diminished Lewis acidity with Ni(II) on the breakdown of the alkylperoxy intermediate initiated by the removal of the C-3 proton (cf. Scheme 1), the primary kinetic isotope effect (KIE) on cofactor formation in Ni(II)-HPAO was measured. Studies were initiated by expressing apo-HPAO in *E. coli* that had been cultured in metal-free medium supplemented with 3,5-[$^2H_2$]tyrosine. To determine the level of deuterium incorporated into the protein, preparations of apo-HPAO harboring tyrosines with and without a heavy label were digested with trypsin and the resulting mixture of peptides was analyzed by MALDI mass spectrometry. From the measured masses of the peptides derived from the unlabeled protein, the identities of the fragments were assigned on the basis of the specificity of trypsin alone (Table 2). From a comparison of the monoisotopic peaks of the tryptic peptides derived from the unlabeled and labeled proteins, the measured shifts in mass corresponded to an increase of 2 mass units for every di-deuterated tyrosine introduced. Furthermore, careful inspection of the mass spectrum of the tryptic digest derived from the deuterated protein showed the absence of any contributions from the isotopic envelopes of peptides containing unlabeled tyrosines, indicating the near 100% random incorporation of the 3,5-[$^2H_2$]tyrosine at every position. With assurance that the deuterium probes had been successfully incorporated into the tyrosyl ring at position 405, the unlabeled and labeled proteins were individually reconstituted with Ni(II) and the rate constants for cofactor formation compared. The observed spectral changes upon the aeration of the Ni(II) forms of the isotopically distinct forms of the protein were identical (data not shown), as were the rates for TPQ biogenesis (Table 1). These data rule out the decay of the peroxy intermediate as the rate-limiting step in cofactor formation in Ni(II)-HPAO.

The depressed Lewis acidity of Ni(II) could potentially impede the Michael addition of the metal-bound hydroxide to dopa quinone during cofactor biogenesis. If this step is indeed rate-limiting, the dopa quinone intermediate would be expected to accumulate in the active site during the Ni(II)-catalyzed transformation. TPQ biogenesis was initiated in Ni(II)-HPAO by the introduction of air, and aliquots were removed at designated times for subsequent reaction with

Table 2: Tryptic Peptides from Digestion of Apo-HPAO[a]

peptide	measured MH^+ for [^{1}H]Tyr	measured MH^+ for [^{2}H]Tyr	calcd MH^+ for [^{1}H]Tyr	$\Delta m/z$
HANF**Y**PK	876.42	878.42	876.43	2.00
FHIGF$\overline{N}$**Y**R	1053.48	1055.52	1053.53	2.04
VIFIDIP$\overline{N}$R	1086.60	1086.60	1086.63	
LQQALV**YY**R	1153.60	1157.64	1153.63	4.04
KVIFIDIP$\overline{N}\overline{R}$	1214.69	1214.70	1214.73	
KVIFIDIPNRR	1370.79	1370.80	1370.83	
GVIH**Y**LDAHFSDR	1529.69	1531.73	1529.75	2.04
V**Y**CD$\overline{P}$WTIG**Y**DER	1616.63	1620.67	1616.71	4.04
L$\overline{Y}$PSGDHVP$\overline{Q}$WSGDGVR	1869.79	1871.83	1869.88	2.04
V$\overline{G}$AMRPEAPPINVTQPEGVSFK	2324.08	2324.13	2324.21	
ALETVQPILTVEDLCSTEEVVIR	2458.14	2458.18	2458.28	

[a] Monoisotopic values for tryptic peptides of HPAO grown in media containing tyrosine with natural isotopic abundance or 3,5-$^2H_2$ label.

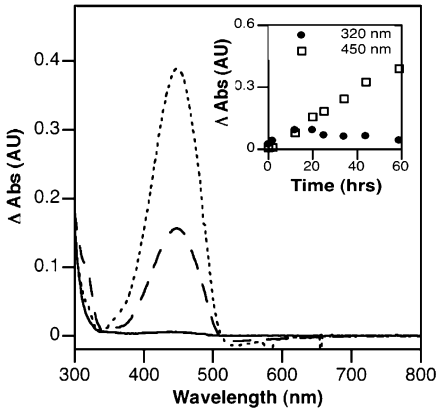

FIGURE 5: Reaction of phenylhydrazine with Ni(II)-HPAO during TPQ biogenesis. The difference spectra that are shown represent the final spectrum following a 30 min reaction of phenylhydrazine with Ni(II)-HPAO 0 (—), 20 (— — —), and 60 h (- - -) after initiation of cofactor formation in air-saturated buffer. The initial spectrum of the cofactor-containing enzyme prior to the addition of phenylhydrazine has been subtracted. The inset shows the time dependence of phenylhydrazones at 320 and 450 nm. Reactions were performed under the following conditions: 27 μM HPAO, 23 μM Ni(II), 0.34 mM phenylhydrazine, and 50 mM HEPES at pH 8.1.

phenylhydrazine to trap all quinones present as their corresponding phenylhydrazones (Figure 5). Early in the time frame of cofactor biogenesis, the phenylhydrazone for TPQ was seen (λ_{max} = 450 nm). With increasing time, a peak at 320 nm could be detected in addition to the phenylhydrazone for TPQ. A precursor—product relationship was displayed between the unidentified quinone and TPQ. The phenylhydrazone of the transient quinone (320 nm) displayed spectral properties similar to that for 2-phenylazo-3,4-dimethylphenol (λ_{max} = 325 nm) (*30*). These data most plausibly indicate the trapping of dopa quinone that has accumulated at the active site of HPAO, suggesting that its hydration during Ni(II)-catalyzed TPQ biogenesis is at least partially rate-limiting.

DISCUSSION

Ni(II) was supplied to apo-HPAO and found to catalyze the biogenesis of TPQ under ambient conditions (Figure 1). Among the nickel-containing enzymes, urease and glyoxalase I catalyze the isomerization and hydrolysis of their respective substrates and each contains a Ni(II) ion bound by a combination of nitrogen and oxygen ligands (*31*), analogous to the active site ligands available for metal binding to HPAO. Alternatively, superoxide dismutase, hydrogenase, carbon monoxide dehydrogenase, and acetyl-coenzyme A synthase catalyze redox reactions requiring a bound nickel ion to cycle between different oxidation states. Since Ni(II) in a N/O-rich environment is relatively redox inert, a reoccurring theme appears to be the evolution of nickel centers containing thiolate and amidate ligands to achieve a redox active site that is accessible in biological systems (*31*—*33*). Therefore, the Ni(II)-catalyzed six-electron oxidation of the precursor tyrosine (Y405) to TPQ is unlikely to involve a formal change in valence state at the metal site. We sought to understand the mechanism by which Ni(II) can serve as a catalyst for the monooxygenation of tyrosine in an active site that is devoid of thiolate or amidate ligands.

Mechanism of Ni(II)-Catalyzed TPQ Biogenesis. The crystal structures of the Zn(II)- and Cu(II)-reconstituted forms of HPAO showed the unprocessed tyrosine axially bound to metal and poised for cofactor biogenesis (*8*, *9*). The recent structure of the Ni(II)-substituted form of the mature AGAO revealed a metal ion chelated by conserved histidines, an equatorial water, and two axial waters in an octahedral geometry (*34*). Since the principal geometries for Ni(II) are square planar and octahedral, it is likely that the precursor tyrosine replaces an axial water ligand to the metal to form an initial tyrosinate—Ni(II) complex (Scheme 1).

We note that some fraction of the exogenously added nickel gave rise to a broad absorbance feature that was unaltered by prebinding of Zn(II) at the active site (Figure 2), implicating some metal binding outside of the active site. An even broader absorbing feature emerged following the introduction of air to the Ni(II)-Y405V mutant (Figure 3B). Considering that the mutant is incapable of producing cofactor, the oxygen-dependent chromophore (334 nm) was deemed to be associated with oxidative chemistry not relevant to TPQ biogenesis. Contributions from the product of an oxidative side reaction were also evident upon the aeration of the nickel-bound WT HPAO, as judged by the appearance of the 334 nm band in addition to that for TPQ (Figure 3A). The coordination of Ni(II) by thiolate ligands (surface accessible residues in HPAO being C122, C193, C336, and C478) (*8*) gives rise to a characteristic optical signature (at 357 nm, ϵ = 2900 cm^{-1} M^{-1}, and at 407 nm, ϵ = 3500 cm^{-1} M^{-1}) (*35*) and is presumed to be the source of the absorbance feature associated with the binding of Ni(II) to the surface of HPAO in the absence of oxygen. Further, transition metal—thiolate complexes are frequently air sensitive and subject to sulfur—ligand oxidation to form cysteine oxygenates (*36*), offering one possible explanation for further changes in absorbance following aeration of the metalated samples. To minimize reaction from extraneous

Ni(II) sites in selected experiments (e.g., EPR), apo-HPAO was reconstituted with Ni(II) in the absence of oxygen and subsequently washed to remove unbound or weakly bound metal prior to the introduction of oxygen.

Following the addition of O_2 to Ni(II)-HPAO, TPQ appeared at a rate ca. 100-fold slower than that with Cu(II) (Table 1 and Figure 3A). Dissimilar to Cu(II)-catalyzed cofactor biogenesis (*12*), the Ni(II)-dependent reaction did not yield any spectral precursors to TPQ (Figure 3A). Time-resolved EPR spectroscopy of the nickel-bound protein during the production of the quinone cofactor revealed the absence of a transient signal at $g = 2.0$ due to a carbon-based radical (Figure 4). However, a species displaying a signal at $g = 2.3$ emerged over time that was most consistent with a metal-based oxidation generating Ni(III) ($S = {}^1/_2$) (*22*, *23*) or an antiferromagnetically coupled system with $S = 1$ Ni(II) and $S = {}^1/_2$ phenoxyl radical electrons (*24*). This EPR active species appeared to be derived from a very minor, off the reaction path product, as opposed to a transient intermediate during cofactor formation since the quantity of unknown spin amounted to only 3% of the final amount of TPQ. It was concluded that the bulk of the bound nickel remained in an EPR silent 2+ oxidation state throughout the course of cofactor biogenesis. These findings were incorporated into the mechanism proposed for Ni(II)-catalyzed cofactor biogenesis in HPAO (Scheme 1). As shown, TPQ formation is proposed to commence with the binding of Ni(II) to the histidine triad. By analogy with Cu-(II)-dependent biogenesis, the introduction of air leads to O_2 binding near the metal site (*13*, *37*) and movement of the precursor tyrosine toward the metal. As proposed, the Ni-(II)−tyrosinate complex is oxidized by an outer-sphere electron transfer to dioxygen, generating superoxide anion along with a Ni(II)−tyrosyl radical [possibly stabilized via a Ni(III)−phenolate resonance structure]. The generation of a caged radical pair by electron transfer circumvents the spin restrictions for the oxygenation of tyrosine and allows for the rapid combination of the reduced oxygen species with the unpaired spin on the tyrosyl ring to form an alkyl peroxide intermediate. The subsequent removal of the C-3 ring proton initiates heterolytic O−O bond cleavage and generates dopa quinone, which is then subject to nucleophilic attack by the metal-bound hydroxide to form topa. In the final step, the triol form of the cofactor reduces dioxygen by sequential electron-transfer steps to yield hydrogen peroxide and the oxidized cofactor, TPQ.

Efforts To Identify the Rate-Limiting Step(s) in Ni(II)-Catalyzed TPQ Biogenesis. As illustrated, the nickel ion must promote a combination of monooxygenase, hydration, and oxidase reactions to catalyze the overall oxidation of a neighboring tyrosine to the quinone cofactor. The properties that will contribute to the competency of Ni(II) to carry out these functions include its Lewis acidity, reduction potential, and electrostatic stabilization capabilities. To define the principle function of Ni(II) in this series of reactions, we sought to clarify the rate-limiting step(s) for cofactor biogenesis.

As an oxidase, HPAO couples the two-electron reduction of dioxygen to hydrogen peroxide to the oxidation of amine substrates. The oxidation of the intermediate, reduced cofactor (aminoquinol) has been shown to contribute to rate limitation during catalytic turnover (*20*, *21*; K. Takahashi and J. Klinman, unpublished data). The proximity of the mononuclear Cu(II) center was thought to enhance the rate of oxidation of the aminoquinol more than 4 orders of magnitude compared to the oxidation of the 6-amino-4-ethylresorcinol analogue alone (*20*). These data, together with the high activity of the cobalt-substituted enzyme (*20*, *21*), emphasize the importance of the metal ion for the stabilization of the superoxide anion intermediate by electrostatic stabilization. The substitution of Ni(II) for Cu(II) could perform a similar role, leading to the expectation of a measurable k_{cat} value. As shown in Table 1, k_{cat} is respectable, though reduced ca. 40-fold from that of the native enzyme. This is similar to observations for AGAO, where replacement of Cu(II) with Ni(II) resulted in a 50−100-fold decrease in k_{cat} (*34*). Most germane for this study is the fact that the value of k_{cat} in Table 1 represents a lower limit for the oxidation of the aminoquinol during catalytic turnover. Since the aminoquinol and trihydroxyphenylalanine forms of the cofactor have similar reduction potentials (*29*), the measured k_{cat} can be used as an indirect reporter of the capacity of Ni(II)-HPAO to facilitate the oxidation of the triol to TPQ during cofactor biogenesis. The finding that k_{cat} remained 10^4 times faster than k_{TPQ} for Ni(II)-HPAO (Table 1) led us to eliminate the oxidase reaction as the rate-limiting step in TPQ biogenesis with Ni(II).

The hydration of dopa quinone to topa is highly dependent on the Lewis acidity of the metal, which determines the overall availability of the bound hydroxide poised for nucleophilic attack (Scheme 1). Although this step has not been considered rate-limiting for Cu(II)-catalyzed TPQ biogenesis in HPAO, the hydration of dopa quinone is at least slow enough with respect to the oxidation of the triol form of the cofactor to permit detection of the dopa quinone intermediate during time-resolved crystallographic studies of TPQ biogenesis in AGAO (*9*). Since Ni(II) ($pK_a = 9.4$) is an inferior Lewis acid relative to Cu(II) ($pK_a = 7.5$) (*28*), this substitution could impede the Michael addition of metal hydroxide and result in the accumulation of the dopa quinone intermediate. The absolute requirement for the adjacent metal-bound hydroxide in the hydration of dopa quinone was demonstrated in recent studies utilizing engineered catechols tethered to metal-coordinating units (*38*). Moreover, the observed rate for the conversion of 4-{2-[bis(2-pyridylmethyl)amino]ethylaminomethyl}-1,2-benzenediol to the corresponding hydroxyquinone was found to be significantly slower with Ni(II) than with Cu(II). Last, the kinetic pH−rate profiles for metal-dependent hydroxyquinone formation established a dependence on the pK_a of the metal-coordinated water. To investigate whether the Michael addition of Ni-(II)-OH was rate-limiting in TPQ biogenesis on the enzyme, apo-HPAO was reconstituted with Ni(II) and reacted with phenylhydrazine at various times throughout cofactor formation to capture dopa quinone present in the active site as the stable phenylhydrazone. As expected, the phenylhydrazone for TPQ (450 nm) steadily increased over time (Figure 5). In addition, a second band consistent with the phenylhydrazone of a transient quinone was observed at 320 nm. Since the trapped quinone exhibited a precursor−product relationship with respect to TPQ and its phenylhydrazone had a λ_{max} similar to that for 2-phenylazo-3,4-dimethylphenol (325 nm) (*30*), the Michael addition of the Ni(II)-OH was concluded to be a likely partially rate-limiting step in cofactor formation.

Transition metals can promote O−O bond heterolysis of coordinated alkyl peroxides by acting as a Lewis acid to enhance the electrophilicity of the departing oxygen atom. Thus, the substitution of Ni(II) could also have been expected to have a detrimental effect on the metal-assisted cleavage of the alkyl peroxide intermediate (Scheme 1). To assess if the breakdown of the peroxo intermediate was the rate-limiting step in Ni(II)-catalyzed cofactor formation, the impact of metal substitution on O−O cleavage was determined by the measurement of a primary KIE on k_{TPQ}. These studies entailed the preparation of apo-HPAO containing randomly incorporated 3,5-[$^2H_2$]tyrosine. Mass spectrometric analysis of the tryptic fragments derived from the labeled protein revealed essentially 100% incorporation of the deuterium label (Table 2) and permitted the full expression of a KIE on cofactor formation. However, a comparison of k_{TPQ} measured for the unlabeled and di-deuterated forms of Ni(II)-HPAO indicated little or no difference (Table 1), eliminating the breakdown of the peroxy intermediate as the rate-limiting step in Ni(II)-catalyzed cofactor formation.

Although the hydration of the dopa quinone intermediate is suggested to be partially rate-limiting for Ni(II)-catalyzed TPQ biogenesis in HPAO, the measured rates for the modeled reaction at a similar pH far exceeded k_{TPQ} (*38*); this indicated that the true bottleneck for Ni(II)-dependent cofactor biogenesis was likely to be further upstream. Experimental (*11*, *12*) and theoretical (*16*) studies point to the insertion of the first oxygen atom into the precursor tyrosine to form an alkyl peroxide intermediate as the rate-limiting step during Cu(II)-catalyzed TPQ biogenesis. One important difference between Cu(II)- and Ni(II)-dependent biogenesis is the extreme difficulty in achieving a Ni(II)−tyrosine resonance form that is capable of combination with O_2, i.e., a Ni(I)−tyrosine radical species [E_m for Ni(II)/(I) = −1.16 V (vs NHE) for metal complexes with nitrogen and oxygen ligands (*27*)]. A more feasible mechanism is one in which the complexation of the tyrosine precursor to Ni(II) facilitates an outer-sphere electron transfer to generate transiently a tyrosine radical and superoxide anion. From the Marcus formalism for outer-sphere electron transfer (*39*), the rate constant for electron transfer (k_{ET}) is dependent on driving force ($\Delta G°$), which is related to the difference in the standard reduction potential ($E°$) for the two half-reactions by the Nerst equation. The standard reduction potential for the one-electron reduction of dioxygen to superoxide is −0.16 V (vs NHE) (*14*). Typical potentials for the Ni(III)/(II) couple bound in an oxygen- or nitrogen-rich environment are in excess of +0.86 V (vs NHE) (*40*, *41*), which is expected to render the divalent cation redox inert. Likewise, the oxidation of free tyrosine is difficult as demonstrated by the E_m of +0.93V (vs NHE) for the TyrO$^•$/TyrOH couple (*42*). Like the proposed mechanism for Cu(II)-dependent TPQ biogenesis, the coordination of the deprotonated precursor tyrosine to Ni(II) must be the key. We propose that the coordination of tyrosine to Ni(II) facilitates the removal of an electron from the Ni(II)−phenolate unit, as demonstrated by the suppressed reduction potential for the Ni(II)−phenoxyl radical/Ni(II)−phenolate couple (E_m = +0.66 V vs NHE) (*24*) compared to that of free tyrosyl radical. We note that a Ni(II)−phenolate intermediate remains a very poor one-electron reductant with respect to molecular oxygen and this exchange is expected to be extremely endergonic. As such, the uphill nature of a direct electron transfer from the Ni(II)−phenolate unit to dioxygen may well constitute the major rate-limiting step in cofactor formation. The finding that Ni(II)−phenolate complexes absorb at a similar λ_{max} (400−450 nm) as TPQ but with a reduced extinction coefficient ($\epsilon \cong 900\ M^{-1}\ cm^{-1}$) (*24*) may explain our inability to detect this species during Ni(II)-supported biogenesis.

Oxygenation by Mononuclear Ni(II) Centers. We note that, to date, only two enzymes have been demonstrated to possess Ni(II)-dependent oxygenase activities, MomA (*43*) and aci-reductone dioxygenase (ARD) (*44*). ARD is proposed to incorporate both atoms from dioxygen into 1,2-dihydroxy-3-keto-5-methylthiopentene via an initial single-electron transfer from the Ni(II)-coordinated dianionic substrate to molecular oxygen. Here, the nickel ion was proposed to persist in the 2+ state throughout the catalytic cycle and function in a nonredox capacity (*45*). In the case of MomA, the monooxygenation of 1,3,6,8-tetrahydroxynaphthalene to the quinone-containing product, flaviolin, was tentatively postulated to be mediated by a redox-cycling transition metal (*43*). However, the metal dependence of monooxygenation by MomA is promiscuous, and the putative metal binding motifs characteristic of cupin proteins are devoid of conserved cysteines. Thus, it seems unlikely that the active site of MomA would be conducive to redox chemistry at a Ni(II) site, and a more likely mechanism is one in which the deprotonated substrate transfers an electron directly to molecular oxygen. This conclusion is corroborated by the susceptibility of the anionic forms of aci-reductone and polyhydroxynaphthalenes to air oxidation by nonenzymatic reactions (*44*, *46*). One critical distinction between ARD and MomA catalysis versus TPQ biogenesis is that the substrates in the former case are already activated for the reduction of dioxygen by direct electron transfer. This points again to an essential role in HPAO for a Ni(II)−tyrosinate complex which is proposed to reduce the redox potential of the tyrosine ring to a range that can support outer-sphere electron transfer to a prebound molecule of O_2. Key questions that remain are, first, why Ni(II) is so much more effective than Co(II) in TPQ biogenesis and, second, why Zn(II) is completely inert. The latter observation almost certainly arises from the closed shell property of Zn(II), while the former may reflect the greater propensity for Co(II) to do oxidative chemistry unrelated to TPQ biogenesis. Future experimental and computational studies may be able to provide insight into the perplexing aspects of metal specificity in the copper amine oxidases.

CONCLUSION

The copper amine oxidases utilize a transition metal to carry out several different reactions within a single active site. Because of the dual-functional nature of amine oxidase in catalysis and biogenesis, the optimal transition metal must be able to provide the proper balance of redox properties, Lewis acidity, and electrostatic stabilization capabilities. Herein, we demonstrate the unexpected versatility of Ni(II) in replacing Cu(II) as a catalyst for TPQ biogenesis in HPAO, although at a reduced rate and, likely, by an altered mechanism. Despite being an inferior Lewis acid relative to Cu(II), divalent nickel was concluded to facilitate the O−O bond cleavage of a postulated peroxy intermediate and

electron transfer from trihydroxyphenylalanine to molecular oxygen. Evidence was presented for the possible accumulation of dopa quinone, which implicated the Ni(II)-dependent hydration of this intermediate as a partially rate-determining step. The principal rate-limiting step for TPQ biogenesis by Ni(II)-HPAO was proposed to involve an initial outer-sphere electron transfer from the Ni(II)−tyrosinate complex to molecular oxygen, a process made possible by the reduced redox potential of the Ni(II)−tyrosinate unit and its role in stabilizing a superoxide intermediate.

ACKNOWLEDGMENT

We thank Dr. Michael Marletta and Dr. Vittal Yachandra for the use of their anaerobic glovebox and EPR spectrophotometer, respectively. We also thank Dr. Ke-Qing Ling for providing rate constants for the Ni(II)-catalyzed reaction for the conversion of a model catechol to hydroxyquinone. We acknowledge Dr. Junko Yano and Dr. Olafur Magnusson for valuable technical assistance in acquiring EPR spectra.

NOTE ADDED IN PROOF

Subsequent to submission of this paper, a report appeared of Ni(II)-supported biogenesis of TPQ (Okajima et al., (2005) *Biochemistry 44*, 12041−12048).

REFERENCES

1. Mure, M., Mills, S. A., and Klinman, J. P. (2002) Catalytic mechanism of the topa quinone containing copper amine oxidases, *Biochemistry 41*, 9269−9278.
2. McIntire, W. S., and Hartman, C. (1993) in *Principles and applications of quinoproteins* (Davidson, V. L., Ed.) pp 97−171, Marcel Dekker, New York.
3. O'Sullivan, J., Unzeta, M., Healy, J., O'Sullivan, M. I., Davey, G., and Tipton, K. F. (2004) Semicarbazide-sensitive amine oxidases: Enzymes with quite a lot to do, *Neurotoxicology 25*, 303−315.
4. Janes, S. M., Mu, D., Wemmer, D., Smith, A. J., Kaur, S., Maltby, D., Burlingame, A. L., and Klinman, J. P. (1990) A new redox cofactor in eukaryotic enzymes: 6-Hydroxydopa at the active site of bovine serum amine oxidase, *Science 248*, 981−987.
5. Cai, D. Y., and Klinman, J. P. (1994) Evidence for a self-catalytic mechanism of 2,4,5-trihydroxyphenylalanine quinone biogenesis in yeast copper amine oxidase, *J. Biol. Chem. 269*, 32039−32042.
6. Ruggiero, C. E., and Dooley, D. M. (1999) Stoichiometry of the topa quinone biogenesis reaction in copper amine oxidases, *Biochemistry 38*, 2892−2898.
7. Cai, D. Y., Williams, N. K., and Klinman, J. P. (1997) Effect of metal on 2,4,5-trihydroxyphenylalanine (Topa) quinone biogenesis in the *Hansenula polymorpha* copper amine oxidase, *J. Biol. Chem. 272*, 19277−19281.
8. Chen, Z. W., Schwartz, B., Williams, N. K., Li, R. B., Klinman, J. P., and Mathews, F. S. (2000) Crystal structure at 2.5 Å resolution of zinc-substituted copper amine oxidase of *Hansenula polymorpha* expressed in *Escherichia coli*, *Biochemistry 39*, 9709−9717.
9. Kim, M., Okajima, T., Kishishita, S., Yoshimura, M., Kawamori, A., Tanizawa, K., and Yamaguchi, H. (2002) X-ray snapshots of quinone cofactor biogenesis in bacterial copper amine oxidase, *Nat. Struct. Biol. 9*, 591−596.
10. Ruggiero, C. E., and Dooley, D. M. (1997) Mechanistic studies of topa quinone biogenesis in phenethylamine oxidase, *Biochemistry 36*, 1953−1959.
11. Schwartz, B., Dove, J. E., and Klinman, J. P. (2000) Kinetic analysis of oxygen utilization during cofactor biogenesis in a copper-containing amine oxidase from yeast, *Biochemistry 39*, 3699−3707.
12. Dove, J. E., Schwartz, B., Williams, N. K., and Klinman, J. P. (2000) Investigation of spectroscopic intermediates during copper-binding and TPQ formation in wild-type and active-site mutants of a copper-containing amine oxidase from yeast, *Biochemistry 39*, 3690−3698.
13. DuBois, J. L., and Klinman, J. P. (2005) The nature of O_2 reactivity leading to topa quinone in the copper amine oxidase from *Hansenula polymorpha* and its relationship to catalytic turnover, *Biochemistry 44*, 11381−11388.
14. Bertini, I., Gray, H. B., Lippard, S. J., and Valentine, J. S. (1994) *Bioinorganic chemistry*, University Science Books, New York.
15. Halfen, J. A., Jazdzewski, B. A., Mahapatra, S., Berreau, L. M., Wilkinson, E. C., Que, L., and Tolman, W. B. (1997) Synthetic models of the inactive copper(II)-tyrosinate and active copper-(II)-tyrosyl radical forms of galactose and glyoxal oxidases, *J. Am. Chem. Soc. 119*, 8217−8227.
16. Prabhakar, R., and Siegbahn, P. E. M. (2004) A theoretical study of the mechanism for the biogenesis of cofactor topaquinone in copper amine oxidases, *J. Am. Chem. Soc. 126*, 3996−4006.
17. Matsuzaki, R., Fukui, T., Sato, H., Ozaki, Y., and Tanizawa, K. (1994) Generation of the topa quinone cofactor in bacterial monoamine-oxidase by cupric ion-dependent autooxidation of a specific tyrosyl residue, *FEBS Lett. 351*, 360−364.
18. Su, Q. J., and Klinman, J. P. (1998) Probing the mechanism of proton coupled electron transfer to dioxygen: The oxidative half-reaction of bovine serum amine oxidase, *Biochemistry 37*, 12513−12525.
19. Cai, D. Y., and Klinman, J. P. (1994) Copper amine oxidase: Heterologous expression, purification, and characterization of an active enzyme in *Saccharomyces cerevisiae*, *Biochemistry 33*, 7647−7653.
20. Mills, S. A., and Klinman, J. P. (2000) Evidence against reduction of Cu^{2+} to Cu^{+} during dioxygen activation in a copper amine oxidase from yeast, *J. Am. Chem. Soc. 122*, 9897−9904.
21. Mills, S. A., Goto, Y., Su, Q. J., Plastino, J., and Klinman, J. P. (2002) Mechanistic comparison of the cobalt-substituted and wild-type copper amine oxidase from *Hansenula polymorpha*, *Biochemistry 41*, 10577−10584.
22. Lappin, A. G., Murray, C. K., and Margerum, D. W. (1978) Electron-paramagnetic resonance studies of nickel(III)-oligopeptide complexes, *Inorg. Chem. 17*, 1630−1634.
23. Haines, R. I., and McAuley, A. (1981) Synthesis and reactions of nickel(III) complexes, *Coord. Chem. Rev. 39*, 77−119.
24. Shimazaki, Y., Huth, S., Karasawa, S., Hirota, S., Naruta, Y., and Yamauchi, O. (2004) Nickel(II)-phenoxyl radical complexes: Structure-radical stability relationship, *Inorg. Chem. 43*, 7816−7822.
25. DuBois, J. L., and Klinman, J. P. (2005) Mechanism of post-translational quinone formation in copper amine oxidases and its relationship to the catalytic turnover, *Arch. Biochem. Biophys. 433*, 255−265.
26. Verhagen, M. F., Meussen, E. T., and Hagen, W. R. (1995) On the reduction potentials of Fe and Cu−Zn containing superoxide dismutase, *Biochim. Biophys. Acta 1244*, 99−103.
27. Gomes, L., Pereira, E., and de Castro, B. (2000) Nickel(II) complexes with N_2OS and N_2S_2 co-ordination spheres: Reduction and spectroscopic study of the corresponding Ni(I) complexes, *J. Chem. Soc., Dalton Trans. 8*, 1373−1379.
28. Yatsimirksii, K. B., and Vasil'ev, P. V. (1960) *Instability constants of complex compounds*, Pergamon Elmsford, New York.
29. Mure, M., and Klinman, J. P. (1993) Synthesis and spectroscopic characterization of model compounds for the active-site cofactor in copper amine oxidases, *J. Am. Chem. Soc. 115*, 7117−7127.
30. Ospenson, J. N. (1951) Some studies on azo dyes. II, *Acta Chem. Scand. 5*, 491−509.
31. Mulrooney, S. B., and Hausinger, R. P. (2003) Nickel uptake and utilization by microorganisms, *FEMS Microbiol. Rev. 27*, 239−261.
32. Kruger, H. J., Peng, G., and Holm, R. H. (1991) Low-potential nickel(III,II) complexes: New systems based on tetradentate amidate thiolate ligands and the influence of ligand structure on potentials in relation to the nickel site in [NiFe]-hydrogenases, *Inorg. Chem. 30*, 734−742.
33. Maroney, M. J. (1999) Structure/function relationships in nickel metallobiochemistry, *Curr. Opin. Chem. Biol. 3*, 188−199.
34. Kishishita, S., Okajima, T., Kim, M., Yamaguchi, H., Hirota, S., Suzuki, S., Kuroda, S., Tanizawa, K., and Mure, M. (2003) Role of copper ion in bacterial copper amine oxidase: Spectroscopic and crystallographic studies of metal-substituted enzymes, *J. Am. Chem. Soc. 125*, 1041−1055.
35. Dietrich, H., Maret, W., Kozlowski, H., and Zeppezauer, M. (1981) Active site-specifically reconstituted nickel(II) horse liver alcohol

dehydrogenase: Optical spectra of binary and ternary complexes with coenzymes, coenzyme analogs, substrates, and inhibitors, *J. Inorg. Biochem. 14*, 297−311.

36. Kaasjager, V. E., Bouwman, E., Gorter, S., Reedijk, J., Grapperhaus, C. A., Reibenspies, J. H., Smee, J. J., Darensbourg, M. Y., Derecskei-Kovacs, A., and Thomson, L. M. (2002) Unique reactivity of a tetradentate N_2S_2 complex of nickel: Intermediates in the production of sulfur oxygenates, *Inorg. Chem. 41*, 1837−1844.
37. Goto, Y., and Klinman, J. P. (2002) Binding of dioxygen to nonmetal sites in proteins: Exploration of the importance of binding site size versus hydrophobicity in the copper amine oxidase from *Hansenula polymorpha*, *Biochemistry 41*, 13637−13643.
38. Ling, K. Q., and Sayre, L. M. (2005) A dopaquinone model that mimics the water addition step of cofactor biogenesis in copper amine oxidases, *J. Am. Chem. Soc. 127*, 4777−4784.
39. Marcus, R. A., and Sutin, N. (1985) Electron transfers in chemistry and biology, *Biochim. Biophys. Acta 811*, 265−322.
40. Nag, K., and Chakravorty, A. (1980) Monovalent, trivalent and tetravalent nickel, *Coord. Chem. Rev. 33*, 87−147.
41. Bhattacharya, S., Mukherjee, R., and Chakravorty, A. (1986) A nickel(III) complex with a NiO_6 coordination sphere, *Inorg. Chem. 25*, 3448−3452.
42. DeFelippis, M. R., Murthy, C. P., Faraggi, M., and Klapper, M. H. (1989) Pulse radiolytic measurement of redox potentials: The tyrosine and tryptophan radicals, *Biochemistry 28*, 4847−4853.
43. Funa, N., Funabashi, M., Yoshimura, E., and Horinouchi, S. (2005) A novel quinone-forming monooxygenase family involved in modification of aromatic polyketides, *J. Biol. Chem. 280*, 14514−14523.
44. Dai, Y., Pochapsky, T. C., and Abeles, R. H. (2001) Mechanistic studies of two dioxygenases in the methionine salvage pathway of *Klebsiella pneumoniae*, *Biochemistry 40*, 6379−6387.
45. Al-Mjeni, F., Ju, T., Pochapsky, T. C., and Maroney, M. J. (2002) XAS investigation of the structure and function of Ni in acireductone dioxygenase, *Biochemistry 41*, 6761−6769.
46. McGovern, E. P., and Bentley, R. (1975) Biosynthesis of flaviolin and 5,8-dihydroxy-2,7-dimethoxy-1,4-naphthoquinone, *Biochemistry 14*, 3138−3143.

BI051176M